Biochemistry

 Volume 35, Number 3 January 23, 1996

Accelerated Publications

Identifying the Physiological Electron Transfer Site of Cytochrome *c* Peroxidase by Structure-Based Engineering†

Mark A. Miller,*,‡ Lois Geren,§ Gye Won Han,‡,|| Aleister Saunders,⊥ James Beasley,⊥ Gary J. Pielak,⊥ Bill Durham,§ Francis Millett,§ and Joseph Kraut‡

Department of Chemistry and Biochemistry, University of California at San Diego, La Jolla, California 92093-0317, Department of Chemistry, University of Arkansas, Fayetteville, Arkansas 72701-1201, and Departments of Chemistry and Biochemistry and Biophysics, University of North Carolina, Chapel Hill, North Carolina 27599-3290

Received October 26, 1995; Revised Manuscript Received December 6, 1995⊗

ABSTRACT: A technique was developed to evaluate whether electron transfer (ET) complexes formed in solution by the cloned cytochrome *c* peroxidase [CcP(MI)] and cytochromes *c* from yeast (yCc) and horse (hCc) are structurally similar to those seen in the respective crystal structures. Site-directed mutagenesis was used to convert the sole Cys of the parent enzyme (Cys 128) to Ala, and a Cys residue was introduced at position 193 of CcP(MI), the point of closest contact between CcP(MI) and yCc in the crystal structure. Cys 193 was then modified with a bulky sulfhydryl reagent, 3-(*N*-maleimidylpropionyl)-biocytin (MPB), to prevent yCc from binding at the site seen in the crystal. The MPB modification has no effect on overall enzyme structure but causes 20−100-fold decreases in transient and steady-state ET reaction rates with yCc. The MPB modification causes only 2−3-fold decreases in ET reaction rates with hCc, however. This differential effect is predicted by modeling studies based on the crystal structures and indicates that solution phase ET complexes closely resemble the crystalline complexes. The low rate of catalysis of the MPB-enzyme was constant for yCc in buffers of 20−160 mM ionic strength. This indicates that the low affinity complex formed between CcP(MI) and yCc at low ionic strength is not reactive in ET.

The cytochrome *c* peroxidase (CcP)[1] :cytochrome *c* (Cc) redox pair has been widely studied as a model for long distance electron transfer (ET) reactions. The reaction of peroxide with ferric CcP converts the enzyme to compound I (Bosshard et al., 1990), which has two oxidized sites: an oxy-ferryl heme (Fe^{IV}=O) and a stable free radical at Trp 191 ($Trp^{\bullet,+}$). ET from Cc^{II} reduces both oxidized sites of compound I rapidly, despite a separation of ≥17 Å between the hemes of CcP and Cc (Pelletier & Kraut, 1992; Finzel et al., 1984).

The mechanism of compound I reduction is a matter of ongoing debate. A large body of evidence indicates that

‡ University of California at San Diego.
§ University of Arkansas.
|| Present address: Department of Chemistry, University of California, Los Angeles.
⊥ University of North Carolina, Chapel Hill.

† This work was supported by National Science Foundation grant MCB 94-29845 to M.A.M. and J.K., and National Institutes of Health Grants GM 20488 to F.M. and B.D., and GM 42501 to G.J.P.
⊗ Abstract published in *Advance ACS Abstracts,* January 1, 1996.

[1] Abbreviations: ET, electron transfer; CcP, cytochrome *c* peroxidase from bakers' yeast; CcP(MI), a cloned yeast cytochrome *c* peroxidase expressed in *Escherichia coli* as described in Fishel et al. (1987); yCc, cytochrome *c* from yeast *Saccharomyces cerevisiae*; hCc, cytochrome *c* from horse heart; MPB, 3-(*N*-maleimidylpropionyl)biocytin; Fe^{IV}=O, oxy-ferryl heme; $Trp^{\bullet,+}$, the indolyl radical formed at Trp 191 of CcP; DTNB, 5,5′-dithiobis(2-nitrobenzoic acid); Ru-Cc, cytochrome *c* labeled with a ruthenium bipyridine group covalently attached at a Lys or Cys residue; Zn(por)-Cc and Zn(por)-CcP, cytochrome *c* and cytochrome *c* peroxidase with Zn-heme in place of the normal iron heme; Zn(por•), zinc porphyrin cation radical.

0006-2960/96/0435-667$12.00/0

reduction occurs by the ordered mechanism shown in Scheme 1 (eqs 1−3 below):

Scheme 1

$$CcP^{IV}{=}O;Trp^{\bullet,+} + Cc^{II} \xrightarrow{k_a} CcP^{IV}{=}O + Cc^{III} \quad (1)$$

$$CcP^{IV}{=}O + H^+ \rightleftharpoons^{K_{FR}} CcP^{III}{-}OH;Trp^{+,\bullet} \quad (2)$$

$$CcP^{III}{-}OH;Trp^{+,\bullet} + Cc^{II} + H^+ \xrightarrow{k_b} CcP^{III} + Cc^{III} + H_2O \quad (3)$$

In Scheme 1, Cc^{II} reduces $Trp^{\bullet,+}$ initially, leaving the oxyferryl heme (eq 1). An internal ET reaction regenerates $Trp^{\bullet,+}$ and reduces the heme back to the ferric state (eq 2).[2] A second molecule of Cc^{II} then reduces $Trp^{\bullet,+}$ to regenerate ferric CcP (eq 3) (Geren et al., 1991; Hahm et al., 1992, 1993, 1994; Liu et al., 1994). Consistent with Scheme 1, reduction of the oxyferryl heme is absolutely dependent on a readily oxidized Trp at position 191 (Mauro et al., 1988; Miller et al., 1995) and is influenced by the equilibrium between the oxy-ferryl heme and $Trp^{\bullet,+}$(Liu et al., 1994; Miller et al., 1994). Scheme 1 requires only one binding site for Cc^{II} and is consistent with the crystal structures of complexes formed between a cloned CcP [CcP(MI); Fishel et al., (1987)][3] and cytochromes *c* from horse and yeast (Pelletier & Kraut, 1992). In these complexes, Trp 191 is interposed between the hemes of CcP(MI) and Cc.

Alternatives to Scheme 1 have been proposed. Stopped-flow studies led Erman and co-workers to conclude that at low ionic strength Cc^{II} reduces the oxyferryl center of compound I first, then reduces $Trp^{\bullet,+}$ (Matthis et al., 1995; Nuevo et al., 1993; Summers & Erman, 1988). Independent reduction of the two oxidized sites without equilibration between the oxidized sites has also been proposed (Hazzard & Tollin, 1991; Kang et al., 1977). These mechanisms seem incompatible with the crystal structure of the CcP(MI):Cc^{II} complex, which predicts initial reduction of $Trp^{\bullet,+}$, but are supported by recent evidence for a second, low-affinity Cc binding site (Mauk et al., 1994; Kornblatt & English, 1986; Wang & Margoliash, 1995) if it is assumed that this site is highly reactive (Stemp & Hoffman, 1993; Zhou & Hoffman, 1993, 1994; Zhou et al., 1995).

To elucidate the detailed mechanism of compound I reduction, the relationship between the high affinity CcP:Cc complexes in solution and the CcP(MI):Cc crystal structures must be established, and the possible contribution of a second Cc binding site must be evaluated. Preliminary results suggest that the high affinity complex between CcP and Cc in solution is similar to that seen in the crystal structure (Miller et al., 1994; Wang & Margoliash, 1995; Pappa & Poulos, 1995), but these studies have not resolved between the one- and two-site mechanisms. Toward this end, we created a double mutant of CcP(MI) in which the single cysteine (Cys 128) of the parent enzyme was mutated to Ala, and Ala 193 (the point of closest contact between CcP(MI) and yCc in the crystal structure was mutated to Cys. Cys 193 of the mutant was then modified with 3-(*N*-maleimidyl-propionyl)biocytin (MPB), a bulky sulfhydryl reagent. The effect of this modification on transient and steady-state oxidation of yCc and hCc was then determined.

MATERIALS AND METHODS

Materials. Cytochromes *c* from bakers' yeast (*Saccharomyces cerevisiae*) and horse (type VI) were obtained from Sigma and were used without further purification. 3-(*N*-Maleimidylpropionyl)biocytin (MPB) was obtained from Molecular Probes (Eugene, OR). All other materials were of reagent grade or better.

Enzymes. Mutations were introduced into the CcP(MI) gene by site-directed mutagenesis as described previously (Fishel et al. 1987). To create the double mutant enzyme, Cys 128 was first mutated to Ala. The CcP(MI,A128) enzyme was isolated and purified from cultures of *Escherichia coli* using procedures described elsewhere (Fishel et al., 1987). A second round of mutagenesis was used to convert Ala 193 to Cys. To purify CcP(MI,A128,C193), the free sulfhydryl at Cys 193 must be modified before adding heme to the enzyme. To accomplish this, the enzyme was purified from the crude bacterial homogenate in the presence of 0.5 mM dithiothreitol, apoenzyme was separated from heme-containing enzyme (Miller et al., 1994), the enzyme solution was adjusted to pH 7.6 with 1 N NaOH, and a 5-fold molar excess of MPB was added for 30 min at 4 °C. A standard DTNB assay (Habeeb, 1972) showed 0.9−1.1 mol of free sulfhydryl/mol of enzyme initially, and no free sulfhydryl after MPB treatment. Heme was added to the apo-MPB-enzyme by standard procedures (Fishel et al., 1987). Crystalline enzyme was dissolved in H_2O/MeOH/HOAc, 50:50:0.5, to a final concentration of 50 μM, and the samples were analyzed by the Scripps Research Institute Mass Spectrometry Facility, La Jolla, CA. Purified parental CcP(MI) contained a major species (84%) MW = 33 727, and a minor species (16%) MW = 33 595. This is consistent with the predicted molecular weight of 33 732 for CcP(MI) and 33 601 for enzyme lacking the N-terminal Met residue. The MPB double mutant contained two comparable species: a major one (73%) MW = 34 252 and a second one (15%) MW = 34 119. These two species are 524 and 525 mass units greater than the corresponding peaks of CcP(MI), respectively, in agreement with the predicted molecular weight of 524 for the MPB moiety. An additional minor component (7.7%), of molecular weight 34 033, was identified in the sample. This component is presumed to represent maleimidyl-enzyme that lacks the biotinyl moiety. The predicted molecular weight of such a species is 34 041. The 8 mass unit difference between the predicted and observed molecular weights of the minor species is statistically significant and indicates that a second modification must accompany loss of the biotinyl moiety.

Details of the MPB double mutant enzyme crystal structure will be presented elsewhere (G. W. Han et al., manuscript

[2] It is important to note, however, that the ET rate from Cc^{II} to the oxy-ferryl heme is faster than the overall equilibrium between Trp 191 and the oxy-ferryl heme (eq 2) at pH ≥ 7.0 (Liu et al., 1994; Ho et al., 1984). Under these conditions, a charge transfer state may replace the Trp 191 radical, or the indole ring may simply provide a medium for superexchange between the two hemes. This is discussed further in Miller et al. (1995).

[3] We have distinguished explicitly between CcP from bakers' yeast and the cloned CcP(MI). The two enzymes are essentially identical in overall structure and function, but differ at position 53, which is Thr in CcP and Ile in CcP(MI), and at position 152, which is Asp in CcP and Gly in CcP(MI). CcP is used in cases where data exist for both enzymes.

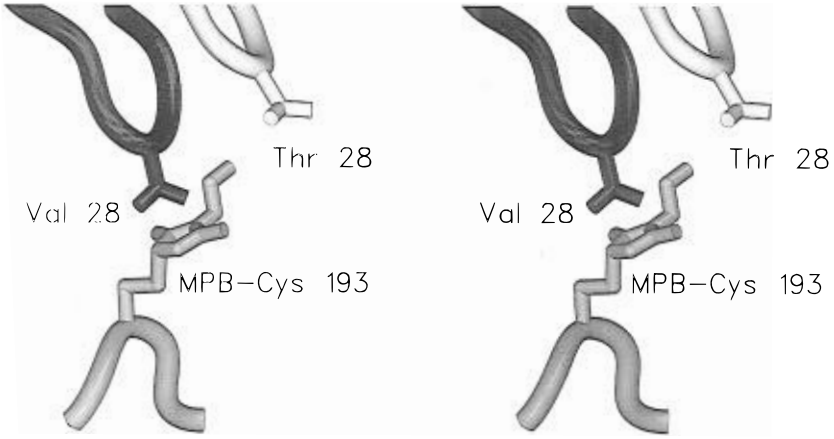

FIGURE 1: Stereo model showing a predicted interaction of the MPB mutant CcP(MI) with yCc and hCc. A model of MPB-CcP(MI,-A128,C193) was superimposed upon the coordinates for the backbone atoms of CcP(MI) in the CcP(MI):yCc complex (Pelletier & Kraut, 1992) using a least-squares minimization program. CcP(MI) and the malemidyl moiety at Cys 193 are shown in dark gray, Val 28 of yCc is shown in black, and Thr 28 of hCc is shown in white. Rotation of the Cys side chain about the $C_\alpha-C_\beta$ bond produces two orientations for the MPB moiety that are favorable for CcP(MI) alone. When modeled in the CcP(MI):yCc crystal structure, the orientation shown here places the MPB moiety 1.6 Å from the predicted position of yCc-Val 28, but 5.5 Å from the predicted position of hCc-Thr 28. The model predicts even greater conflicts between the MPB moiety and yCc-Val 28 in the second orientation (not shown) but no conflicts with hCc are predicted.

in preparation). The MPB derivative was disordered in the crystal, presumably due to formation of both *R*- and *S*-isomers when the sulfhydryl of Cys 193 reacts with the maleimidyl moiety. The mutations have little effect on the overall fold of the enzyme, as the rms deviation of all backbone atoms in residues 2−294 from the CcP(MI) parent is 0.3 Å. The coordinates for the MPB mutant have been deposited in the Brookhaven Data Bank under the four letter access code 1CYF.

Kinetics. Measurements of transient unimolecular and bimolecular ET rates were conducted according to established procedures, using Ru-bipy derivatives of hCc and yCc (Geren et al., 1991; Hahm et al., 1992, 1993, 1994; Liu et al., 1994, 1995). Steady-state kinetic measurements were made in 5 mM sodium phosphate buffer, pH 6.0, adjusted to the desired ionic strength with NaCl, as described elsewhere (Miller et al., 1995).

RESULTS

Computer Simulations of CcP:Cc Complexes. The MPB moiety was disordered in the crystal structure (see Materials and Methods), so computer simulations were used to predict the effect of both MPB-Cys 193 isomers on the CcP(MI):yCc and CcP(MI):hCc complexes seen in the crystal (Pelletier & Kraut, 1992). Models were constructed using standard geometry constraints (Tronrud & Ten Eyck, 1987) and superimposed on the coordinates for CcP(MI) in the CcP-(MI):yCc or CcP(MI):hCc complexes. These studies reveal that the maleimidyl ring of the MPB mutant causes severe steric conflicts within the CcP(MI):yCc complex (Figure 1). For both isomers, the maleimidyl ring makes close contacts with yCc side chains in all positions obtained by rotation of the MPB-Cys 193 side chain about the $C_\alpha-C_\beta$ bond. Thus, the CcP(MI):yCc complex seen in the crystal cannot be formed when the maleimidyl group is attached. In contrast, steric conflicts are absent from the CcP(MI):hCc complex (Figure 1), because the distance between residue 193 of CcP-(MI) and the hCc heme is much larger than the analogous distance in the CcP(MI):yCc complex (Pelletier & Kraut, 1992; Figure 2). Some conformations of the biocytinyl moiety of MPB are predicted to cause conflicts with hCc, but these conflicts can be avoided by rotation about C−C bonds. Thus, the MPB moiety will not prevent formation of the CcP(MI):hCc complex seen in the crystal, but it may increase the free energy of the complex.

Transient Kinetics of Compound I Reduction. The effect of the MPB moiety on ET was quantified by measuring intracomplex ET rates for CcP and the MPB mutant. Intracomplex ET from Cc^{II} to compound I is too fast to be measured by conventional mixing techniques but can be measured if compound I and Cc^{III} are mixed prior to reduction of Cc^{III} (Geren et al., 1991). This is accomplished by linking a ruthenium bipyridine moiety to yCc (Ru-yCc) or hCc (Ru-hCc) and photoreducing Cc^{III} according to the mechanism shown in Scheme 2.

Scheme 2

$$Ru^{II}\text{-}Cc^{III} \overset{h\nu}{\rightleftharpoons} Ru^{II*}\text{-}Cc^{III} \rightleftarrows Ru^{III}\text{-}Cc^{II} \xrightarrow{EDTA} Ru^{II}\text{-}Cc^{II}$$

A laser pulse excites Ru^{II}-Cc^{III} to the luminescent triplet state, Ru^{II*}-Cc^{III}, and the triplet Ru^{II*} ligand reduces the Cc^{III} heme to form Ru^{III}-Cc^{II}. When a sacrificial electron donor such as EDTA is included to prevent the back reaction to re-form Ru^{II}-Cc^{III}, the intermediate Ru^{II}-Cc^{II} accumulates. When Ru^{II}-Cc^{III} is mixed with compound I and photoexcited in the presence of EDTA, ET from the ferrous heme of Ru^{II}-Cc^{II} to compound I can be followed via absorption spectroscopy, where oxidation of Cc^{II} is monitored at 550 nm, and reduction of the oxy-ferryl heme of compound I is monitored at 434 nm, which is an isosbestic point for Cc^{II}/Cc^{III}. This technique has shown that Ru^{II}-Cc^{II} first reduces $Trp^{\bullet,+}$ and then reduces the oxy-ferryl heme (Hahm et al., 1991).

Intracomplex ET from yCc^{II} to $Trp^{\bullet,+}$ of the MPB mutant and CcP was measured at low ionic strength (μ = 3 mM), where essentially all of the Ru-Cc is complexed with compound I. When Ru39-yCc is the substrate, the rate constant for ET (k_{et}) is 92-fold smaller for the MPB-mutant enzyme than for the CcP(MI) parent (Table 1). When Ru27-hCc is the substrate, k_{et} for the MPB mutant is only 2-fold

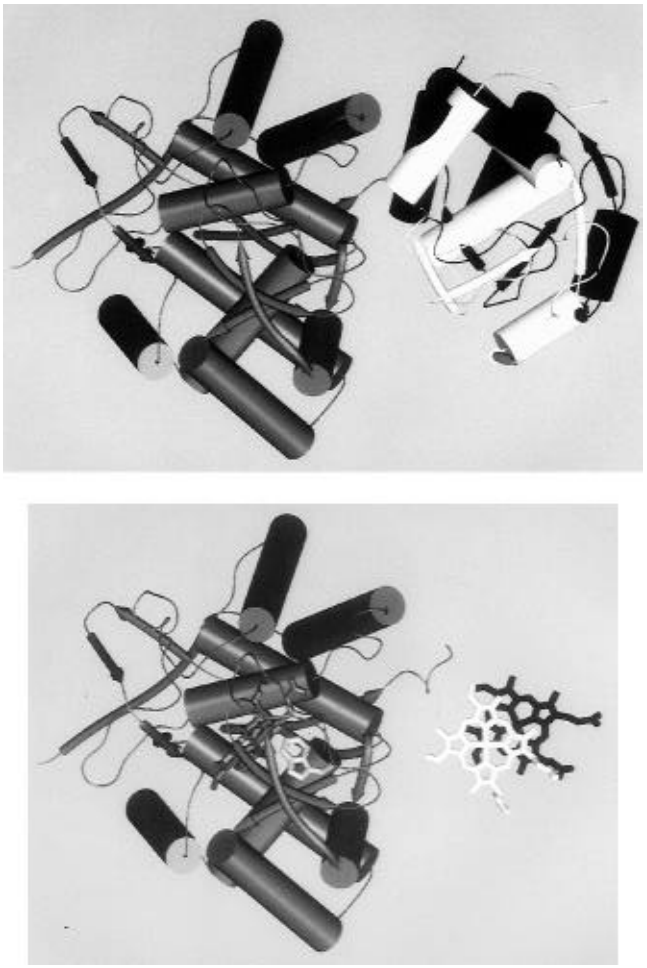

FIGURE 2: Structure models of the ET active binding modes for yCc and hCc at the surface of CcP(MI). The image was created by superimposing peptide backbone atoms of CcP(MI) from models of the crystalline CcP(MI):hCc and CcP(MI):yCc complexes (Pelletier & Kraut, 1992) with a least-squares minimization program. The ribbon trace for CcP(MI) is shown in gray, yCc is shown in white, and hCc is shown in black. In this view, hCc is rotated counterclockwise and then translated upward and into the Z-plane with respect yCc. (Panel A, top) Ribbon traces for yCc bound in Y-mode and hCc bound in H-mode. (Panel B, bottom) The positions of the yCc (black) and hCc (white) hemes are shown relative to CcP(MI) when bound in their respective modes. The CcP(MI)-Trp 191 side chain is shown in light gray.

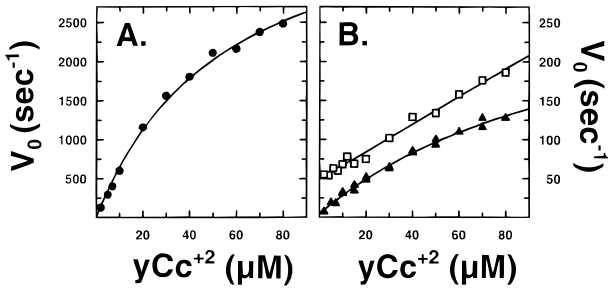

FIGURE 3: yCc dependence of steady-state activity of CcP(MI) at three different ionic strengths. Reactions were conducted as described under Materials and Methods. (Panel A) Initial rate of yCc oxidation at μ = 160 mM. (Panel B) Initial rate of yCc^{II} oxidation at μ = 40 mM (open squares) and μ = 20 mM (solid triangles). Solid lines represent the best fit of the data using the parameters reported in Figure 4.

smaller than the CcP(MI) parent (Table 1).

Intermolecular ET rates were also measured using unmodified Cc^{II} at high ionic strength ($\mu \geq$ 110 mM), where

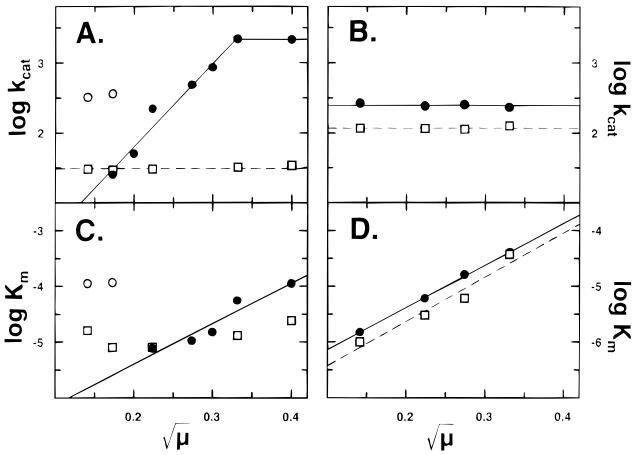

FIGURE 4: Steady-state parameters for oxidation of Cc by CcP(MI) and MPB-CcP(MI,A128,C193). (Panel A) k_{cat} with yCc^{II} as substrate; (panel B) k_{cat} with hCc^{II} as substrate; (panel C) K_m with yCc^{II} as substrate; (panel D) K_m with hCc^{II} as substrate. Solid circles: CcP(MI), low K_m. Open circles: CcP(MI), high K_{m2}. Open squares: MPB-CcP(MI,A128,C193). All reactions were conducted at 25 °C in 5 mM potassium phosphate (pH 6.0) adjusted to the appropriate ionic strength with NaCl by methods described in detail elsewhere (Miller et al., 1995).

binding of Cc^{II} to CcP is weaker and reduction of Trp$^{\bullet,+}$ as well as the oxy-ferryl heme can be completely resolved by stopped flow spectrophotometry (Geren et al., 1993). When compound I is mixed with yCc^{II} or hCc^{II} at high ionic strength, Trp$^{\bullet,+}$ is reduced initially, and the oxyferryl heme is reduced in a lagging phase. The bimolecular rate constants for reduction of Trp$^{\bullet,+}$ (k_a) and the oxyferryl heme (k_b) of the MPB mutant are 20-fold smaller than the CcP parent when yCc^{II} is the donor, but were decreased by only ≈3-fold when hCc^{II} is the donor (Table 1). The bimolecular rate constants k_a and k_b are identical for Ru39-yCc and native yCc, which indicates that the decrease in k_a is not caused by interaction of the ruthenium group attached to yCc with the MPB moiety. Thus, the MPB moiety dramatically decreases the ET rate within the CcP:yCc complex but has a much smaller effect on the ET rate within the CcP:hCc complex.

Despite the small effect of the MPB moiety on k_{et}, other evidence indicates that CcP(MI) and hCc interact near residue 193, as predicted by the crystal structure. When the dissociation rate constant (k_5) and the equilibrium dissociation constant ($K_d = k_5/k_6$) for the CcP(MI):Ru27-hCc complex (eq 4) were determined as described by Liu et al. (1995),

$$\text{CcP(MI):Ru27-hCc}^{II} \underset{k_6}{\overset{k_5}{\rightleftharpoons}} \text{CcP(MI)} + \text{Ru27-hcC}^{II} \quad (4)$$

the values for both parameters are significantly higher for the MPB mutant than for CcP (Table 2). This is consistent with perturbation of the CcP(MI):hCc complex by the MPB-moiety. The Ala 193 → Phe mutation also lowers the affinity of CcP(MI) for hCc (Liu et al., 1994; Erman et al., manuscript in preparation), further indicating that Ala 193 is near the interface of the CcP(MI):hCc complex.

Steady-State Kinetics. We observed a strong correlation between the effect of the MPB moiety on transient ET rates and its effect on steady-state oxidation of yCc^{II} and hCc^{II}. Steady-state oxidation of yCc^{II} is strongly dependent upon ionic strength (Matthis & Erman, 1995; Nuevo et al., 1993), and the effect of the MPB moiety must be considered in this context. For CcP(MI), v_0 is a simple hyperbolic function

Table 1: Kinetic Parameters for ET from yCc to CcP and MPB-CcP(MI,A128,C193)[a]

	pH	k_{et}[b] ($\times 10^{-4}$ s^{-1})	k_{cat}[c] ($\times 10^{-2}$ s^{-1})	k_a[d] ($\times 10^{-7}$ M^{-1} s^{-1})	k_b[e] ($\times 10^{-7}$ M^{-1} s^{-1})	k_{cat}/K_m[c] ($\times 10^{-7}$ M^{-1} s^{-1})
CcP:yCc	6		22	20	3.5	3.8
	7	120[f]		17[g]	2.3[g]	
MPB mutant:yCc	6		0.32 (1.5)	1.0[e] (5)	0.19[e] (5)	0.14 (4)
	7	1.3 (1.1)		0.5[g] (3)	0.10[g] (4)	
CcP:hCc	6	6.1	2.5	20	3.0	0.6
MPB mutant:hCc[f]	6	3.0 (49)	1.2 (47)	8.0 (40)	1.0 (33)	0.6 (100)

[a] Transient ET rates using Ru-bipyridine derivatives of hCc and yCc (Geren et al., 1991; Hahm et al., 1993), and steady-state kinetic measurements were made as described under Materials and Methods. [b] Measured with Ru-39-yCc, in 3 mM sodium phosphate buffer. [c] Measured in 5 mM sodium phosphate buffer, pH 6.0, adjusted to 110 mM ionic strength with NaCl. [d] Bimolecular reduction of Trp 191 radical of compound I measured with stopped flow spectrophotometer. [e] Bimolecular reduction of oxyferryl heme of compound II measured with stopped flow spectrophotometer. [f] Measured in 10 mM MES, 300 mM NaCl. [g] The measurement of this parameter will be described in detail in elsewhere (Geren et al., manuscript in preparation). [h] Measured in 5 mM sodium phosphate, 300 mM NaCl.

Table 2: Kinetics of the Photooxidation Electron Transfer Cycle in the Ru-27-Cc:CcP Complex[a]

	K_d (μM)		k_5 ($\times 10^3$ s^{-1})	
μ (mM)	CcP	MPB-C193	CcP	MPB-C193
12	<1	0.2	1−4	8
22	<1	1	1−4	13
32	<1	2.4	2−5	20
42	<1	4.9	7	32
52	1.0	7.4	14	59
62	1.9	12	21	>70
82	5.5	24		
102	13.5	52		
122	25	78		

[a] The rate constants for the reaction cycle defined in the text were determined in solutions containing 5 μM Ru-27-Cc and 5 μM CcP or MPB-CcP(MI,A128,C193) in 2 mM sodium phosphate, pH 6, adjusted to the indicated ionic strength with 0−120 mM NaCl (Liu et al., 1995). No HOOH or aniline was added. The rate constant k_4, which corresponds to reduction of the Trp 191 radical by Cc^{II}, was 6.1×10^4 s^{-1} for CcP and 3.0×10^4 s^{-1} for MPB-CcP(MI,A128,C193), independent of ionic strength. Experimental error in the reported values is ±15%.

of yCc concentration above $\mu = 100$ mM (Figure 3A). Under these conditions, $k_{cat} \approx 2200$ s^{-1}, and K_m increases as μ is increased to 160 mM (Figure 4A,C). At $\mu < 100$ mM, k_{cat} decreases (Figure 4A), and a simple hyperbola no longer describes the data adequately. Between 90 mM > μ > 50 mM, the dependence of v_0 upon yCc^{II} concentration is best modeled as the sum of a hyperbola and a line. The values of k_{cat} and K_m for the saturable process decrease as the ionic strength decreases, while the slope of the line appears to be constant. At $\mu = 40$ mM, the hyperbolic process is saturated at 2 μM yCc^{II}, giving a linear dependence of v_0 on yCc^{II}, with a *Y*-intercept at 50 s^{-1} (Figure 3B). As the ionic strength is further decreased, the data are best described as a hyperbola with a nonzero intercept. The value of the intercept declines to a value of 6 s^{-1} at $\mu = 20$ mM. At 20 mM ≤ μ ≤ 30 mM, the second process can be characterized as a hyperbola, with $K_{m2} \sim 115$ μM, and a maximal velocity $k_{cat2} \sim 320$ s^{-1} (Figure 3B).

The change in the ionic strength dependence of k_{cat} and the deviation from hyperbolic kinetics at $\mu < 110$ mM are caused by a change in the rate-limiting step. Mutations at the CcP(MI):yCc interface increase k_{cat} at low ionic strength, and lower the ionic strength at which the change in rate-limiting step occurs (M. A. Miller, unpublished observations). These observations indicate that when $\mu < 110$ mM, enzyme turnover is limited by dissociation of yCc from CcP(MI). This is consistent with the observation that yCc dissociation is very slow at low ionic strength Yi et al. (1994).

Under conditions where k_{cat} is limited by product dissociation, a second process contributes to yCc^{II} oxidation. When $\mu > 30$ mM, this process does not saturate at 80 μM yCc^{II} and has a bimolecular rate constant of approximately 1.8×10^6 M^{-1} s^{-1}. At 20 mM ≤ μ ≤ 30 mM, saturation of the second process occurs, suggesting that complex formation between CcP and yCc is involved. The value of k_{cat2} is larger than the rate constant for Cc^{III} dissociation (k_5) at low ionic strength (Yi et al., 1994). Thus, the second process must reflect either an increase in k_5 by substrate-assisted displacement (Corin et al., 1993) or a mechanism where yCc^{II} reacts with the CcP:yCc^{III} complex at low ionic strength. Results of experiments with a variety of CcP(MI) mutants indicate that the former possibility is correct (M. A. Miller, unpublished observations).

The effect of the MPB moiety on steady-state oxidation of yCc^{II} is consistent with this interpretation. The MPB moiety decreases the value of k_{cat} to 31 ± 1 s^{-1} (Figure 4A). The decrease in k_{cat} at 110 mM ionic strength is of the same magnitude as the decrease in the transient electron transfer rate, k_{et} (Table 1). This indicates that electron transfer from the high affinity binding site is rate-limiting under these conditions. The MPB moiety also makes k_{cat} independent of ionic strength from $\mu = 20$ mM to $\mu = 160$ mM, indicating that dissociation of yCc^{III} is not rate-limiting for the MPB mutant enzyme.

Steady-state oxidation of hCc^{II} by CcP(MI) can be described by a simple hyperbolic function at all ionic strengths. The value of k_{cat} is 250 ± 20 s^{-1}, independent of ionic strength (Figure 4B). The value of K_m decreases monotonically with decreasing ionic strength, from 30 μM at $\mu = 110$ mM to 1.5 μM at $\mu = 20$ mM (Figure 4D). The MPB enzyme has a similar ionic strength dependence: $k_{cat} = 115 \pm 5$ s^{-1} (Figure 4B) and K_m decreases monotonically from 30 μM at $\mu = 110$ mM to 1 μM at $\mu = 20$ mM (Figure 4D). The ionic strength independence of k_{cat} for both enzymes is consistent with rapid dissociation of hCc^{III} from CcP at low ionic strength (Yi et al., 1994).

DISCUSSION

The transient ET reactions measured using Ru-Cc and stopped-flow techniques are clearly relevant for steady-state oxidation of yCc^{II} and hCc^{II}. When yCc^{II} is the substrate, the 92-fold decrease in k_{et} for the MPB-mutant relative to CcP is accompanied by a 67-fold decrease in k_{cat} under conditions where electron transfer is rate-limiting. When hCc^{II} is the substrate, electron transfer is also rate limiting, since the 2-fold decrease in k_{et} for the MPB-mutant causes a 2-fold decrease in k_{cat}.

The relationship between k_{et} and k_{cat} can be interpreted in the context of Scheme 1.[4] Single turnover experiments indicate that the initial reduction of $Trp^{\bullet,+}$ is rapid, and the subsequent reduction of the oxyferryl heme is rate-limiting. Reduction of the oxyferryl heme occurs by a two-step mechanism: in the first step, a rapid equilibrium is established between the oxy-ferryl heme and $Trp^{\bullet,+}$ (eq 2).[2] In the second step, rate-limiting ET from yCc^{II} to $Trp^{\bullet,+}$ returns the enzyme to the resting ferric state (eq 3). The rate constant for this reaction (k_{obs}) is a function of the equilibrium constant for CcP(MI):yCc complex formation (K_A), the equilibrium constant for formation of $Trp^{\bullet,+}$ (K_{FR} in eq 2), and the rate of intracomplex ET from yCc to $Trp^{\bullet,+}$ (k_{et}). The relationship is given explicitly as follows:

$$k_{obs} = k_{et}\left(\frac{[yCc^{II}]}{K_A + [yCc^{II}]}\right)\left(\frac{K_{FR}}{K_{FR} + 1}\right) \qquad (5)$$

Equation 5 predicts that changes in k_{et} will cause changes of equal magnitude in k_{obs}. The value of k_{obs} is much smaller than k_{et} because the limiting intermediate [$CcP(MI)^{III}$; $Trp^{+\bullet}$: yCc^{II}] is a small fraction of the total enzyme population. Under steady-state conditions, k_{obs} is the theoretical upper limit for k_{cat}. The observed value of k_{cat} will be less than k_{obs} to the extent that equilibrium binding of yCc^{II} and yCc^{III} to compound I, compound II, and $CcP(MI)^{III}$ lower the concentration of the reactive [$CcP(MI)^{III}$; $Trp^{+\bullet}$:yCc^{II}] complex in solution.

The effect of the MPB moiety on transient and steady-state ET rates indicates that the solution phase ET complexes closely resemble the crystalline CcP(MI):Cc complexes. For the purposes of this discussion, we will define the region of interaction between CcP(MI) and Cc in the crystal structures as a binding site. In the crystal structures, yCc and hCc bind at the same site, but in two distinct orientations, which we shall define as Y-mode and H-mode, respectively. The two modes were thought to arise from differences in crystallization conditions (Pelletier & Kraut, 1992), but the present work indicates that these two modes are also relevant in solution. Thus, the crystal structures retain subtle differences between the CcP(MI):hCc and CcP(MI):yCc complexes that occur in solution (Figure 2A). ET from yCc^{II} is highly efficient, with $k_{et} = 1.2 \times 10^6\ s^{-1}$. This is consistent with Y-mode binding, where the yCc heme is 4 Å from Ala 193 of CcP(MI) and 13 Å from Trp 191 (Figure 2B). ET from hCc^{II} is 20-fold slower, consistent with H-mode binding, where the distance from the hCc heme to Ala 193 of CcP-(MI) and Trp 191 is increased by 6 Å (Figure 2B).

An important prediction of our model is that the MPB moiety will prevent binding in the Y-mode but not binding in the H-mode. Our results are consistent with this prediction: k_{et}, k_{cat}, and k_{cat}/K_m for the reaction of yCc^{II} with the MPB enzyme are all within 4-fold of those observed for hCc^{II} (Table 1), suggesting that the residual activity of yCc^{II} with the MPB-mutant is the result of binding in H-mode. Thus, yCc can bind in the H-mode, although hCc is unable to bind in the Y-mode. Binding of yCc in the H-mode is not detected in the CcP(MI) parent because the H-mode complex is less stable than the Y-mode complex. Binding of yCc is approximately 10-fold stronger than binding of hCc (Matthis & Erman, 1995; Krescheck et al., 1994), so if hCc and yCc have equal affinity in the H-mode, only 10% of the CcP:yCc complex will be in H-mode.

This model for CcP:Cc interaction is significantly different from multisite models proposed by others (Zhou et al., 1995; Zhou & Hoffman, 1993, 1994; Stemp & Hoffman, 1993) because it predicts one well-defined Cc binding site with two possible binding modes. These two binding modes are distinct but should not be viewed as rigid, since recent evidence indicates that two-dimensional diffusion of hCc about CcP is required to achieve a productive ET complex (F. Millett, unpublished observations). Thus, the two binding modes in the crystal represent the energy minima for equilibrium binding of the respective cytochromes, but the orientation of Cc may change before ET occurs. The kinetic results require that the observed ET rate is determined by the initial mode of Cc binding, however.

These data show that physiological ET occurs at the high affinity Cc binding site. This can be reconciled with evidence for a reactive high affinity binding site in covalently cross-linked CcP:Cc complexes (Wang & Margoliash, 1995; Pappa & Poulos, 1995) but differs markedly from results obtained when ET is measured with Zn-heme substituted Cc [Zn(por)-Cc] or CcP [Zn(por)-CcP] (Zhou et al., 1995; Zhou & Hoffman, 1993, 1994; Stemp & Hoffman, 1993). The latter studies report low ET reactivity at the high affinity Cc binding site and high ET reactivity at a second, low affinity binding site. It seems likely that this discrepancy is caused by the effect of Zn substitution on the pathway and reorganization energies for the ET reactions. When quenching of photoexcited ^{3}Zn-Cc by CcP^{III} is used to measure ET, oxidation of Trp 191 does not occur, and therefore the physiological ET pathway does not operate (Zhou & Hoffman, 1993; Stemp & Hoffman, 1993). When ET from Cc^{II} to a Zn porphyrin radical [Zn(por$^\bullet$)-CcP] is measured (Zhou & Hoffman, 1994), activation of the physiological pathway only occurs to the extent that Zn(por$^\bullet$) can oxidize Trp 191. The oxidation potential for Zn(por$^\bullet$) is ~0.25 V lower than for the oxy-ferryl heme (Kaneko et al., 1980). Assuming that equilibrium between Zn(por$^\bullet$) and Trp 191 is rapid relative to ET from yCc, Zn-heme substitution will shift the equilibrium constant K_{FR} in eq 2 ~10^4-fold to the left (that is, $K_{FR(Zn)}/K_{FR(Fe)} = 10^{-4}$). Thus Zn-heme substitution will decrease k_{obs} in eq 5 by 10^4. It is also significant that the reorganization energy for reduction of the oxyferryl heme is much higher than that for Zn(por$^\bullet$) reduction (Gray & Malmström, 1989). The relatively high reorganization energy for reduction of the oxyferryl heme may actually prevent competing ET reactions of the type measured using Zn-hemes. This could explain the evolutionary selection of iron porphyrins for use in enzymes designed to prevent random discharge of a highly oxidized metal center.

The results provide no evidence that a second, low affinity Cc binding site contributes to ET from yCc^{II} to CcP(MI). The value of k_{cat} for yCc^{II} oxidation by the MPB mutant enzyme is constant down to 20 mM ionic strength, where the putative low-affinity Cc binding site is expected to contribute significantly to k_{cat} (Zhou & Hoffman, 1994). It

[4] The mechanism in Scheme 1 cannot be readily reconciled with stopped-flow data suggesting that yCc^{II} reduces the oxy-ferryl heme before $Trp^{\bullet,+}$ (Matthis et al., 1995). While the reaction observed in the stopped-flow experiment is consistent with oxidation of 2 mol of yCc^{II} per mol of compound I, reduction of $Trp^{\bullet,+}$ observed by other techniques cannot be ruled out because the reaction is complete before the stopped flow measurements begin.

is probable that the second, low affinity binding site for yCc (Mauk et al., 1994) plays a non-ET role in the catalytic mechanism of CcP, however. The phenomena of substrate-assisted displacement (Yi et al., 1994) and the unusual ionic strength dependence of k_{cat} and K_m for yCc^{II} oxidation by CcP (Figure 3; Matthis & Erman, 1995) can be explained by assuming that yCc binding at the low affinity site increases the rate of dissociation at the high affinity site (Corin et al., 1993). The existence of this unreactive binding site is probably serendipitous, since it does not contribute to catalysis at physiological ionic strength (Tollin et al., 1993).

ACKNOWLEDGMENT

We are grateful to Sunny Kim and Chuan Chen for outstanding technical assistance.

REFERENCES

Bosshard, H. R., Anni, H., & Yonetani, T. (1990) in *Peroxidases in Chemistry and Biology* (Everse, J., Everse, K. E., Grisham, M. B., Eds.) Vol. 2, Chapter 3, CRC Press, Boca Raton, FL.

Corin, A. F., Hake, R. F., McLendon, G., Hazzard, J. T., & Tollin, G. (1993) *Biochemistry 32*, 2756−2762.

Fishel, L. A., Villafranca, J. E., Mauro, J. M., & Kraut, J. (1987) *Biochemistry 26*, 351−360.

Geren, L., Hahm, S., Durham, B., & Millett, F. (1991) *Biochemistry 30*, 9450−9457.

Gray, H. B., & Malmström, B. G. (1989) *Biochemistry 28*, 7499−7505.

Habeeb, A. F. S. A. (1972) *Methods Enzymol. 25*, 457−464.

Hahm, S., Durham, B., & Millett, F. (1992) *Biochemistry 30*, 3472−3477.

Hahm, S., Durham, B., & Millett, F. (1993) *J. Am. Chem. Soc. 115*, 3372−3373.

Hahm, S., Miller, M. A., Geren, L., Kraut, J., Durham, B., & Millett, F. (1994) *Biochemistry 33*, 1473−1480.

Hazzard, J. T., & Tollin, G. (1991) *J. Am. Chem. Soc. 113*, 8956−8957.

Ho, P. S., Hoffman, B. M., Solomon, N., Kang, C. H., & Margoliash, E. (1984) *Biochemistry 23*, 4122−4128.

Kaneko, Y., Tamura, M., & Yamazaki, Y. (1980) *Biochemistry 19*, 5795−5799.

Kang, C. H., Ferguson-Miller, S., & Margoliash, E. (1977) *J. Biol. Chem. 252*, 919−926.

Kornblatt, J. A., & English, A. M. (1986) *Eur. J. Biochem. 155*, 505−511.

Krescheck, G. L., Vitello, L. B., & Erman, J. E. (1995) *Biochemistry 34*, 8398−8405.

Liu, R.-Q., Hahm, S., Miller, M. A., Geren, L., Hibdon, S., Kraut, J., Durham, B., & Millett, F. (1994) *Biochemistry 33*, 8678−8685.

Liu, R.-Q., Hahm, S., Miller, M. A., Durham, B., & Millett, F. (1995) *Biochemistry 34*, 973−983.

Matthis, A., & Erman, J. E. (1995) *Biochemistry 34*, 9985−9990.

Matthis, A. L., Vitello, L. B., Erman, J. E. (1995) *Biochemistry 34*, 9991−9999

Mauk, M. R., Ferrer, J. C., & Mauk, A. G. (1994) *Biochemistry 33*, 12609−12614.

Miller, M. A., Hahm, S., Liu, R.-Q., Geren, L., Hibdon, S., Kraut, J., Durham, B., & Millett, F. (1994) *Biochemistry 33*, 8686−8693.

Miller, M. A., Erman, J. E., & Vitello, L. B. (1995) *Biochemistry 34*, 12048−12058.

Nuevo, M. R., Chu, H.-H., Vitello, L., & Erman, J. E. (1993) *J. Am. Chem. Soc. 115*, 5873−5874.

Pelletier, H., & Kraut, J. (1992) *Science 258*, 1748−1755.

Pappa, H. S., & Poulos, T. L. (1995) *Biochemistry 34*, 6573−6580.

Stemp, E. A., & Hoffman, B. M. (1993) *Biochemistry 32*, 10848−10865.

Summers, F. E., & Erman, J. E. (1988) *J. Biol. Chem. 263*, 14267−14275.

Tollin, G., Hurley, J. K., Hazzard, J. T., & Meyer, T. E. (1993) *Biophys. Chem. 48*, 259−279.

Tronrud, T. E., Ten Eyck, L. F., & Matthews, B. W. (1987) *Acta Crystallogr. A43*, 489.

Wang, Y., & Margoliash, E. (1995) *Biochemistry 34*, 1948−1958.

Yi, Y., Erman, J. E., & Satterlee, J. D. (1994) *Biochemistry 33*, 12032−12041.

Zhou, J., & Hoffman, B. M. (1993) *J. Am Chem. Soc. 115*, 11008−11009.

Zhou, J., & Hoffman, B. M. (1994) *Science 265*, 1693−1696.

Zhou, J. S., Nocek, J. M., DeVan, M. L., & Hoffman, B. M. (1995) *Science 269*, 204−207.

BI952557A